第27卷 第10期
2006年10月
焊 接 学 报
TRANSACTIONS OF THE CHINA WELDING INSTITUTION
Vol.27 No.10
October 2006

温度与镀层对Sn—Cu—Ni无铅钎料润湿性能的影响

王俭辛[1]， 薛松柏[1]， 韩宗杰[1]， 汪 宁[1]， 禹胜林[2]
（1 南京航空航天大学 材料科学与技术学院，南京 210016；
2 中国电子科技集团第十四研究所，南京 210013）

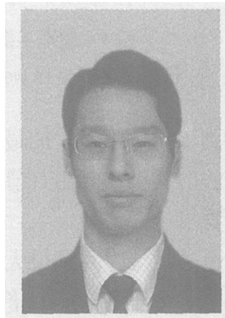
王俭辛

摘 要：采用润湿平衡法测定了在不同试验温度下Sn—Cu—Ni无铅钎料在Cu，Au/Ni/Cu，SnBi/Cu三种基板上的润湿时间和润湿力，研究了钎焊温度对Sn—Cu—Ni无铅钎料在不同基板上润湿性能的影响。结果表明，温度升高使Sn—Cu—Ni无铅钎料的表面张力减小，能显著缩短钎料在铜片上的润湿时间，提高润湿力；Ni/Au或SnBi等镀层能显著降低钎料/基板界面张力，因此Sn—Cu—Ni无铅钎料在Au/Ni/Cu或SnBi/Cu基板上的润湿性能优于在Cu基板上的润湿性能。

关键词：无铅钎料；Sn—Cu—Ni；润湿性；镀层
中图分类号：TG454 文献标识码：A 文章编号：0253—360X(2006)10—053—04

0 序 言

传统的Sn—Pb钎料以其优异的性能和低廉的成本，一直在电子产品的制造中起着重要的作用。近年来，基于人们对使用Sn—Pb钎料危害的认识以及对环境保护的重视，不得不选择无铅钎料作为其替代品[1,2]。遍全球范围已研究和开发出的几十种无铅钎料合金中，基本上都是在Sn—Ag，Sn—Cu，Sn—Bi和Sn—Zn等基础上通过添加少量或微量的第三种、第四种金属元素形成的三元、四元或多元合金体系[3,4]。目前已公认Sn—Ag—Cu系列是再流焊工艺中的主流合金[4~6]，而在波峰焊方面更多的是考虑Sn—Cu系作为Sn—Pb钎料的替代品[6,7]。

Sn—Cu钎料成本较低，作为波峰焊用无铅钎料的应用范围正在不断扩大。但是其熔点偏高，润湿性能不够理想，因此不少研究者提出了一些可行的改善措施，譬如添加微量的Ni，Ag，Au，Ge，In等元素来提高钎料的润湿性能和力学性能[4,6,8]。Sn—Cu—Ni作为Sn—Cu的改进产品，在波峰焊时可以减少焊锡渣的形成和焊点“桥连”现象的产生，特别是可以减轻对印刷电路基板上Cu的溶蚀[6,8]，同时还可以使其润湿性能得到明显的改善。迄今为止，有关Sn—Cu—Ni钎料润湿性的研究尚不多见，对于Sn—Cu—Ni钎料在合金镀层上润湿性的研究更是鲜见报道。文中主要针对Sn—Cu—Ni钎料在波峰焊条件下，采用润湿平衡法测定了钎料在不同基板上的润湿时间和润湿力，研究了钎焊温度以及Ni/Au，SnBi镀层对Sn—Cu—Ni钎料润湿性能的影响规律。

收稿日期：2006—07—29
基金项目：2006年江苏省“六大人才高峰”资助项目

1 试验条件

1.1 试验材料与设备

以Sn—0.5Cu—0.05Ni无铅钎料为研究对象，根据润湿平衡法原理，采用日本Rhesca公司的SAT—5100型可焊性测试仪进行润湿试验。标准试片规格为30 mm×5 mm×0.3 mm，试片有无镀层（纯铜）、Ni/Au镀层、SnBi镀层三种。

1.2 试验原理及方法

试验步骤按照日本工业标准JIS Z3198—4—2003的规定进行。熔融钎料的温度分别预置为240 ℃，250 ℃，260 ℃，270 ℃，280 ℃，试验中添加美国Alpha Metal公司生产的Rosin Free 800型免清洗钎剂。将铜片以4 mm/s的速度垂直浸入熔融钎料中，浸入深度为2 mm，保持时间为10 s，铜片从浸入熔融钎料的瞬间开始，试验设备显示值随时间的动态变化如图1所示。

铜片刚浸入熔融钎料时润湿还没有发生，主要受向上的浮力作用，而使曲线向下出现负值。随后铜片开始被润湿，受到熔融钎料对它向下的润湿力，该润湿力先克服浮力到达图中②点，并随润湿过程逐渐增大，至④点达到最大稳定值。将试验设备所测得的最大稳定值即最大合力加上铜片受到的浮力

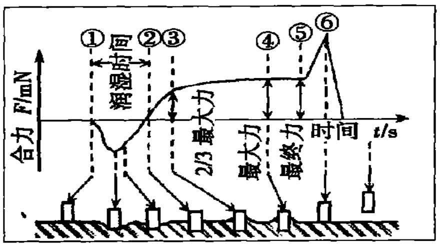

图 1　润湿平衡法的润湿曲线

Fig. 1　Profile of wetting balance method

即得到该熔体对铜片的最大润湿力。图 1 所示润湿平衡法的润湿曲线由计算机自动记录显示, 并保存在计算机中。

通过润湿时间和最大合力两个参数可对钎料在基板上的润湿性进行评价。润湿时间 t_0 为图 1 中①～②之间的时间, 最大合力为④对应的力。润湿时间越短、最大合力越大则表明润湿性越好。对于某种钎料在某种基板上的润湿时间 t_0, 目前国际通用的标准均为美国电子工业标准 IPC/EIA J—STD—003B 2004, 该标准中对于波峰焊的润湿时间的推荐值为 $t_0 \leqslant 1$ s。

2　结果与讨论

2.1　试验温度与镀层对润湿时间 t_0 的影响

分别按 1.2 节中预置的 5 种温度, 测定 Sn—Cu—Ni 钎料在 3 种基板上的润湿性能, 每次试验重复 5 次, 取其平均值。试验结果如图 2 所示。

图 2a 是钎料在 5 种温度下对 Cu 基板的润湿曲线, 240 ℃时 t_0 高达 8 s 之多, 润湿性较差; 温度上升至 250 ℃时, 润湿性显著改善, t_0 急剧下降至 2.2 s, 最大合力也增加了 2 倍; 温度继续上升, 润湿时间 t_0 平稳下降, 到 270 ℃时, t_0 已达到 1 s 左右, 此时已达到美国电子工业标准 IPC/EIA J—STD—003B 2004 对于波峰焊润湿时间的推荐值 $t_0 \leqslant 1$ s 的要求。

图 2b, 图 2c 分别是钎料对 Au/Ni/Cu、SnBi/Cu 基板的润湿曲线, t_0 随温度变化的趋势虽然与图 2a 一致, 但是在相同温度下具有更优异的润湿性, 特别是在较低温度下改善效果更为明显, 这一结果有力地说明了“镀层”的作用和意义。润湿曲线在峰底存在一水平线段后才上行, 这是因为试片浸入钎料静止时, 并没有立即发生润湿, 而是有一个“过程”, 试验温度越高, 此“过程”越短。当温度达到 260 ℃时, 此水平线段消失, Sn—Cu—Ni 钎料在 Ni/Au 上润湿性最好, 且 t_0 在 1 s 左右, 如图 2d 所示。

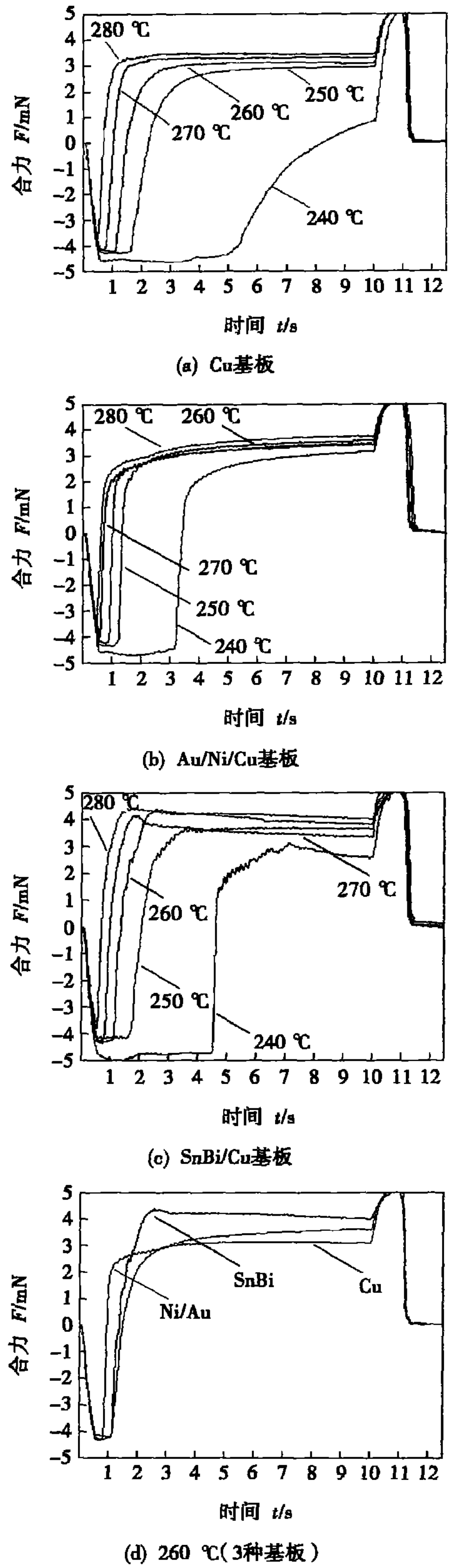

图 2　Sn—Cu—Ni 钎料润湿曲线

Fig. 2　Profiles of wettability of Sn-Cu-Ni solder

Sn—Cu—Ni 钎料在三种基板上的润湿时间依次为 Ni/Au<SnBi<Cu, 说明在 Ni/Au 镀层上润湿性最好, 在 SnBi 镀层上润湿性次之, 在 Cu 上的润湿性

相对最差。试验温度较低时，三种基板上的 t_0 相差较大，试验温度升高，此差距逐渐减少，当试验温度达到或超过 270 ℃时，t_0 基本上已趋于一致，如图 3 所示。

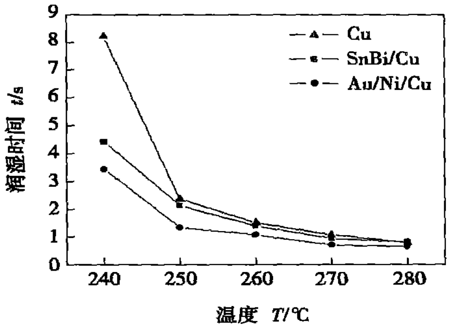

图 3　钎料在不同镀层的润湿时间

Fig. 3　Wetting times of solder on different coatings with different temperatures

钎料对基板的润湿程度取决于熔融钎料的表面张力，而表面张力除了和物质的本性以及所接触邻相的性质有关以外，还与温度有着密切的联系。物质的表面张力通常随着温度的升高而降低，这是因为温度升高时液体体积膨胀，分子间距增大，削弱了体相分子对表面层分子的作用力；同时温度升高后，气相蒸气压变大，密度增加，气相分子对液体表面分子作用增强，这些都使表面张力下降。液体表面张力 γ 与温度 T 的关系为

$$\gamma=\frac{k(T_c-T-\tau)}{(M/\rho)^{2/3}},\tag{1}$$

式中：M 为液体的摩尔质量；ρ 为液体的密度；k 为经验常数；T_c 为表面张力为零时的临界温度；τ 通常取 6K。

由上式可知，随着温度的升高，熔融钎料的表面张力不断减小，这在钎焊过程中有助于提高钎料对基板的润湿性。

从扩散的角度来看，钎焊的过程也是钎料与基板互相扩散的过程，钎焊温度越高，原子活性越强，界面处原子扩散越剧烈，润湿所需时间也随之缩短。

已有研究表明[9]，基板材料 Cu 与钎料中 Sn 的反应速度较快，会生成 Cu_6Sn_5 金属间化合物。在实际生产中，常在 Cu 基板上镀上保护层以防止 Cu_6Sn_5 金属间化合物的生成并提高润湿性能，因此镀层应有良好的稳定性，能抑制扩散和界面反应，并具有足够的强度以传递应力，故文中选取了在实际生产中应用较多的 Ni/Au 和 SnBi 镀层进行润湿性能研究。Ni/Au 表面处理技术中涂敷的 Ni 具有很多优点，如表面平滑、稳定性高及可钎焊性较好，并且在波峰焊时桥连现象少。在润湿过程中，稳定性高的 Ni 层的存在，能够阻挡铜向钎料中的迁移，避免润湿界面金属间化合物的过厚生成，保证基板与钎料形成良好的冶金结合，从而提高了钎料的润湿性能。虽然 Ni 能够形成比 Cu 稳定的多的钎焊连接，但它容易氧化，而 Au 层主要起防止 Ni 氧化的作用。SnBi 合金镀层表面结晶致密，空隙率小故抗氧化力增强，从而提高了钎料对基板的润湿性。

对于铜基板来说，Sn—Ag—Cu 钎料在 260 ℃时就有较好的润湿性，已完全满足波峰焊中 $t_0\leqslant 1$ s 的要求[10]。但是，由于 Sn—Cu—Ni 钎料的熔点较 Sn—Ag—Cu 高出 10 ℃左右，因此在相同温度下，润湿性稍逊一筹，接近 270 ℃时，才具有足够良好的润湿性能，即达到 $t_0\leqslant 1$ s 的要求。

2.2　试验温度与镀层对最大合力 F_{max} 的影响

图 4 反映了最大合力 F_{max} 随温度与镀层的变化趋势。在 240 ℃时，钎料对 Cu 基板的润湿力很低，温度上升至 250 ℃后，最大合力 F_{max} 急剧增大了 3 倍之多。随着试验温度的升高，最大合力 F_{max} 也增大，这与图 2 中的趋势形成对应，说明此时提高温度不仅可加快润湿，而且有利于提高润湿力。但温度继续升高，对润湿力的提高作用不是十分明显，当试验温度达到或超过 270 ℃时，最大合力 F_{max} 基本上已趋于稳定，如图 4 所示。

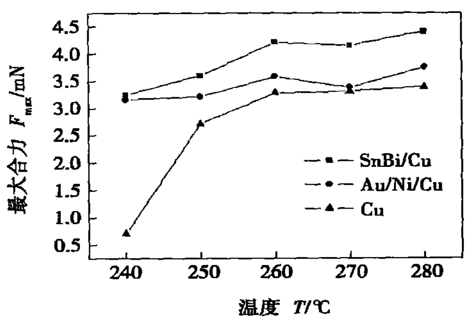

图 4　钎料在不同镀层上的最大合力

Fig. 4　Variety of F_{max} of solder on different coatings with different temperatures

润湿力可以用来定性地研究熔融钎料/基板界面张力，图 5 是采用钎剂保护条件下钎料在母材上的界面张力示意图。

根据 Young—Dupre 方程

$$\gamma_{lg}\cos\theta=\gamma_{gs}-\gamma_{ls},\tag{2}$$

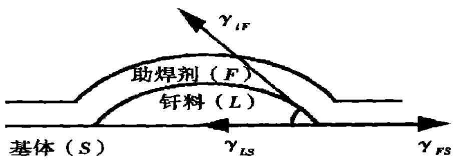

图 5 使用钎剂条件下的界面张力示意图

Fig. 5 Schematic diagram of interfacial tension using flux

式中：γ_{lg} 为钎料表面张力；θ 为钎料—基板—空气三相界面接触角；γ_{gs}为基板表面张力；γ_{ls}为钎料/基板界面张力。润湿力为

$$F_W = L\gamma_{lg}\cos\theta = L(\gamma_{gs} - \gamma_{ls}), \tag{3}$$

式中：L 为铜片浸入钎料中的周长。

由于润湿平衡曲线纵轴表示的力 F 为钎料作用在铜片上的合力，ρgV 为钎料对铜片的浮力，可得

$$F = F_W - \rho gV = L(\gamma_{gs} - \gamma_{ls}) - \rho gV。 \tag{4}$$

试验中各铜片浸入深度一样，浮力都相等，所以润湿平衡曲线纵轴表示的合力 F 的差异只能来源于($\gamma_{gs} - \gamma_{ls}$)值的不同。

对于同种基板，随着温度的升高，F 也随之增大，由此可见升高温度可降低钎料/基板界面张力 γ_{ls}；在相同温度下，钎料对 3 种基板的润湿力排序为 SnBi> Ni/Au> Cu，所以钎料/基板界面张力 γ_{ls}的排序应为 SnBi< Ni/Au< Cu，即在 Cu 基板上镀上 SnBi 或者 Ni/Au 镀层，可降低钎料/基板界面张力，从而改善钎料的润湿性。

3 结 论

（1）随着温度的升高，Sn—Cu—Ni 无铅钎料的表面张力减小，在三种基板上的润湿性能都有显著提高，表现为润湿时间 t_0 逐渐减小，最大合力 F_{max} 逐渐增大。

（2）在相同试验温度下，Sn—Cu—Ni 钎料在 Ni/Au 镀层上的润湿时间最短，在SnBi镀层上的润湿时间次之，在 Cu 基板上的润湿时间相对最长；但是，在SnBi 镀层上的润湿力最大，在 Ni/Au 镀层上的润湿力次之，在 Cu 基板上的润湿力相对最小。

（3）在Cu 基板上镀敷Ni/Au 或SnBi 等镀层，可降低钎料/基板界面张力，从而缩短钎料在基板上的润湿时间，提高润湿力。

参考文献：

[1] Abtew M，Selvaduray G. Lead-free solders in microelectronics[J]. Materials Science and Engineering: R，2000，27(5)：95—141.

[2] Suganuma K. Advances in lead-free electronics soldering[J]. Current Opinion in Solid State and Materials science，2001，5(1)：55—64.

[3] 薛松柏，栗卓新，朱 颖，等. 焊接材料手册[M]，北京：机械工业出版社，2006.

[4] 刘汉诚，汪正平，李宁成，等. 电子制造技术[M]. 姜岩峰，张常年，译. 北京：化学工业出版社，2005.

[5] Wu C M L，Yu Daquan，Law C M T，*et al*. Properties of lead-free solder alloys with rare earth element additions[J]. Materials Science and Engineering: R，2004，44(1)：1—44.

[6] Yoon J W，Lee Y H，Kim D G，*et al*. Intermetallic compound layer growth at the interface between Sn—Cu—Ni solder and Cu substrate[J]. Journal of Alloys and Compounds，2004，381(1—2)：151—157.

[7] Islam M N，Chan Y C. Interfacial reactions of Sn—Cu solder with Ni/Au surface finish on Cu pad during reflow and aging in ball grid array packages[J]. Materials Science and Engineering B，2005，117(3)：246—253.

[8] 菅沼克昭. 无铅焊接技术[M]. 宁晓山，译. 北京：科学出版社，2004.

[9] Yu Da-quan，Wu C M L，Law C M T，*et al*. Intermetallic compounds growth between Sn—3.5Ag lead-free solder and Cu substrate by dipping method[J]. Journal of Alloy and Compounds，2004，380(1—2)：1—8.

[10] 王旭艳. 提高 SnAgCu 无铅钎料润湿性及焊点可靠性的途径的研究[D]. 南京：南京航空航天大学，2006.

作者简介：王俭辛，男，1981 年 11 月出生，博士研究生。主要研究方向为微电子焊接技术及无铅钎料研究，已发表论文 2 篇。
Email：wjx1816@163.com

welding of aluminum alloy. The experiment results demonstrate that the addition of the metal powder enhances the energy coupling efficiency and reduces the power density threshold value during laser deep welding. Such as the reducing rate is about 50% for A2219 alloy. The experiment results also indicate that the powder can enter the weld pool availably only the powder was delivened to the suitable area after laser beam at the surface of a part. The proper quantity of the alloy powder must match with the right power density and energy input, which can assure to obtain good weld appearance. Meanwhile, the addition of the powder can reduce the fluctuation of the laser-induced plasma and maintain its stability effectively in the laser welding. So a stable welding process and good weld appearance can be obtained in the experiments.

Key words: aluminum alloy; metal powder; CO_2 laser welding; laser induced plasma; power density threshold value

Effect of side gas on laser induced plasma during laser deep penetration welding ZHANG Lin-jie[1], ZHANG Jian-xun[1], DUAN Ai-qin[2] (1. State Key Laboratory of Mechanical Behavior for Materials, Xi' an Jiaotong University, Xi' an 710049, China; 2. Beijing Aeronautical Manufacturing Technology Research Institute, Beijing 100024, China). p37—40

Abstract: A two dimensional compressible gas flow model of laser penetretion welding process was founded for a better understanding of the influence of side gas flow conditions on the behavior of laser induced plasma. The distributions of temperature and velocity within plasma plume under different side gas flow conditions were calculated. The shape and size of plasma in laser welding process was studied with high-speed CCD camera. The result shows that laser induced plasma and weld geometry are sensitive to side nozzle height, its inclination angle and side gas flow rate; that cooling effect and assist-gas/plasma-plume momentum ration play an important role in controlling the plasma plume.

Key words: laser deep penatration welding; side assist gas; numerical simulation; high-speed CCD imaging

Mechanical properties and microstructures of QFP micro-joints soldered with diode-laser soldering system HAN Zong-jie, XUE Song-bai, WANG Jian-xin, CHEN Xu (College of Materials Science and Technology, Nanjing University of Aeronautics and Astronautics, Nanjing 210016, China). p41—44

Abstract: Soldering experiments of two kinds of devices QFP32 and QFP48 were carried out using diode-laser soldering system and IR reflow soldering method, and the distribution regulations of the tensile strength of QFP micro-joints with Sn-Pb solder and Sn-Ag-Cu lead-free solder were studied by STR-1000 micro-joints tester, and the characteristics of fracture microstructures of micro-joints were also analyzed by SEM. The results indicate that tensile strength of QFP micro-joints soldered with laser soldering system is larger than that with IR reflow soldering method, and tensile strength of QFP48 micro-joints is larger than that of QFP32 micro-joints. Fracture mechanism of micro-joints soldered with laser soldering system is toughness fracture, while fracture mechanism of micro-joints soldered with IR reflow soldering method includes brittle fracture and toughness fracture.

Key words: diode-laser soldering; QFP devices; mechanical properties of micro-joints; microstructures

Active vision sensing method for weld location by "circle-depth relation" algorithm XU Pei-quan, TANG Xin-hua, LU Jianbo, Yao Shun (School of Material Science and Engineering, Shanghai Jiaotong University, Shanghai 200030, China). p45—48

Abstract: Three vital angles were put forward, so the weld could be described by three-dimensional information. On this basis, mathematical model of depth recovery according to "circle-depth relation" algorithm and projection rules was constructed. The relation ship between depth values and off-axis angle γ under gas tungsten arc welding experiment condition was addressed by real experiment and the characteristic points of weld was described and located. Mean square error was used to analyze the recovery precision. The results showed: (1) Depth recovery for butt joint and ramp welded seams realized; (2) Weld can be located very well by using proposed vision sensor based on circular laser trajectory; and proposed vision sensor manifested a promising result with high precision and high efficiency.

Key words: laser cone projection; circular laser trajectory; depth recovery; seam location

Instantaneous energy waveform of short circuiting transition in CO_2 arc welding XUE Jia-xiang, YANG Guo-hua, WANG Zhen-min, LIU Xiao, HONG Sen (College of Mechanical Engineering, South China University of Technology, Guangzhou 510640, China). p49—52, 84

Abstract: The welding process of three arc welding machines had been tested and analyzed with the welding dynamic arc wavelet analyzer developed by the anthers. The experimental results indicate that the instantaneous energy can synthetically reflect the influence of current and voltage on dynamic arc characteristics. To make are ignite successfully, the instantaneous energy should increase to enough high quickly along with the current. In a cycle of short circuting transition during the steady welding process, the instantaneous energy during arc burning should be kept at the constant base, and then it falls to smaller value rapidly, finally, it rises rapidly and completes the short circuit transition. The instantaneous energy falls again rapidly to base after arc re-striking. While arc extinguishing, the instantaneous energy falls slowly to zero and avoids serious impulsion. The experiment results can provide for the foundation to design and control accurately the waveform of the welding current and voltage.

Key words: instantaneous energy; wavelet analysis; repeatability of waveform

Effects of temperature and coatings on wettability of Sn-Cu-Ni lead-free solder WANG Jian-xin[1], XUE Song-bai[1], HAN Zong-jie[1], WANG ning[1], YU Sheng-lin[2] (1. College of Materials Science and Technology, Nanjing University of Aeronautics and Astronautics, Nanjing 210016, China; 2. The 14th Research Insitute, China Eletronics Technology Group Corporation, Nanjing 210013, China). p53—56

Abstract: Wetting times and wetting forces of Sn-Cu-Ni lead-free solder for different temperatures and three kinds of substrates, including Cu, Au/Ni/Cu, and SnBi/Cu, were measured by means of wetting balance method. The effects of soldering temperature on wettability of Sn-Cu-Ni lead-free solder on different substrates were also studied. The results indicate that with the increase of temperature, the surface tension of the lead-free solder decreases, and the wetting times are reduced observably, and the wetting forces are increased evidently. The wettability of solder on Au/Ni/Cu or SnBi/Cu substrate is better than that on Cu substrate owing to the decrease of the interfacial tension between solder and substrate by way of plating Ni/Au or SnBi coating.

Key words: lead-free solder; Sn-Cu-Ni solder; wettability; coating

On-line weld quality inspection based on weld indentation by using servo gun ZHANG Xiao-yun, ZHANG Yan-song, CHEN Guan-long (School of Mechanical Engineering, Shanghai Jiaotong University, Shanghai 200030, China). p57—60

Abstract: Resistance spot welding (RSW) is the primary joining method for car-body assembly. Control and inspection of weld quality have great importance to improve the performance of car. Based on the position feedback characteristics of servo encoder, on-line weld quality inspection method was proposed by using weld indentation. A spot welding experimental system including robot, robot controller, servo gun and weld controller was integrated. The developed measurement program was used to acquie weld indentation on-line, and the measured results was calibrated by PLC displacement control system. The experimental results showed that the acquired weld indentation can reflect the real indentation on the 0.8mm low carbon steel (GMW2). The weld quality inspection rate can meet the demand for real production. The proposed on-line weld quality inspection method can meet the demand of welded joint measurement in real plant environment.

Key words: resistance spot welding; servo gun; weld indentation; on-line inspection

Method of welding groove feature design and weld feature recognition LIU Yong[1], WANG Ke-hong[1], DU Shan-shan[2], XU Yue-lan[1] (1. Material Department of Science & Engineer, Nanjing University of Science & Technology, Nanjing 210094, China; 2. Computer School of Science & Technology, Nanjing University of Science & Technology, Nanjing 210094, China). p61—64

Abstracts: To solve welding workpiece model, it is important to study welding groove feature design. The design requirements of welding groove were analysed in the numeric CAD/CAPP/ROBOTICS integrated welding. The total scheme was desiged to realize the data share between CAD design environment and CAPP/ROBOTICS environment. Firstly a method to model typical welding groove based on groove feature library was given, then a better method to model universal weld groove driving by program developing based on CAD/CAM platform was provided. And the method of welding groove feature and weld feature recognition was put forward. Example proved that it is correct.

Key words: welding groove; feature design; feature recognition

Fracture microstructures and properties of Al-Li alloy brazed joints ZHANG Ling, XUE Song-bai, SHI Huai-jiang, WU Yu-xiu (College of Materials Science and Technology, Nanjing University of Aeronautics and Astronautics, Nanjing 210016, China). p65—68

Abstract: Microstructures of base metal and brazed joints were analyzed using metallographic microscope, SEM and microhardness instrument, and the changing rule of strength of brazed joints was studied by testing microhardness of brazed joints and chemical composition of fracture micro-section. The results show that shape of reinforcing phase of base metal are changed from particle to strip after brazing; there are few defects such as gas pores, slag inclusions, cracks and so on in brazed joints with N_2 atmosphere, which improves mechanical properties of brazed joints effectively, however there are many defects in brazed joints without N_2 atmosphere, which reduces mechanical properties of brazed joints seriously.

Key words: Al-Li alloy; brazed joint; microstructure; microhardness

Intelligent digital control system for CO_2 short circuiting welding FENG Yue-hai[1,2], LIU Jia[2], YIN Shu-yan[2], WANG Ke-hong (1. Department of Materials Science & Engineering, Nanjing University of Science and Technology, Nanjing 210094, China; 2. College of Mechanical Engineer and Applied Electronics Technology, Beijing University of Technology, Beijing 100022, China). p69—72

Abstract: For the shortage of short circuiting transfer for general CO_2 welding machine, based on the hardware system of digital signal processor and microprocessor control unit, the hierarchical intelligent control theory was applied and the hierarchicall intelligent full digital control schematic for CO_2 short circuiting transfer welding was put forward. It integrates the digital PI controller, fuzzy controller and expert system, which make control levels clearer and design scheme easier. The experimental results validate that this system can attain ideal waveform control for CO_2 short-circuit welding, and improve CO_2 welding machine performance, and control welding process intelligently.

Key words: digital control system; gas metal arc welding; hierarchical intelligent control

Numerical analysis of multi-pass welding residual stress for typical closed weld CHEN Hu, GONG Jian-ming, TU Shan-dong (Nanjing University of Technology, Nanjing 210009, China). p73—76

Abstract: Two typical closed weld, circular patch weld and nozzle weld, were modeled and 3-D multi-pass welding simulation were performed using FEM. User subroutine were used to realized the moving Gauss distribution of welding heat source. The thermal cycle and residual stresses distribution were obtained. The results show that